Electron-spin polarization near the Fermi level in *n*-type modulation-doped semiconductor quantum wells

A. L. C. Triques, J. Urdanívia, and F. Iikawa
Instituto de Física Gleb Wataghin, Universidade Estadual de Campinas, 13083-970 Campinas-SP, Brazil

M. Z. Maialle
DFE, Universidade São Francisco, 13251-900 Itatiba-SP, Brazil

J. A. Brum
Instituto de Física Gleb Wataghin, Universidade Estadual de Campinas, 13083-970 Campinas-SP, Brazil

G. Borhgs
IMEC, Kapeldreef 75, B-3001, Leuven, Belgium

(Received 10 August 1998)

We study the spin polarization of optically created electrons near the Fermi energy in an *n*-type modulation-doped single quantum well. In our system the Fermi level is slightly above the second confined conduction subband. The results reveal that electrons optically created close to the Fermi level partially conserve their spin polarization, despite the presence of the electron gas. Data obtained by changing the excitation intensity show that exchange interaction among optically created electrons and holes dominates the spin flip processes in the vicinity of the Fermi edge. [S0163-1829(99)51412-4]

The influence of a two-dimensional (2D) electron or hole gas in the carrier spin relaxation in semiconductor quantum wells (QW's) has been experimentally[1–6] and theoretically[7–11] investigated in recent years. The experimental work explored both continuous-wave (CW) and time-resolved regimes. The CW results showed that the polarization profile (polarization degree as a function of the excitation energy) depends on the electronic structure of the system, the doping level, and the sample quality. It is also well established that the spin relaxation and the polarization profile are given by the combined effects of two factors: the electronic structure and the joint density of states involved in the transitions.[12] The time-resolved results, however, are not conclusive: spin relaxation times of 4 ps[2] as well as 1 ns[3] have been measured for holes in *n*-type-doped QW's while spin relaxation times of 150 ps[2] and 1 ns[4] were found for electrons in *p*-type-doped QW's. Slower spin relaxation was reported for high-energy electrons compared to low-energy electrons in an *n*-type-doped multiple-QW sample. This was attributed to electron-electron interactions.[2]

In doped semiconductor QW's, the Fermi sea is constituted by equal carrier populations in the spin up and spin down states. The optical polarization is therefore dominated by the spin polarization of the minority carriers. For *n*-type-doped samples the hole spin relaxation is a consequence of the valence-band mixing with the scattering of the hole momentum $\vec{k}_h$ connecting the different spin-mixed states. The optical polarization profile is therefore determined by the valence-band structure. Previous studies[2–4] explored the situation where a dense 2D electron (hole) gas is present. In these cases the spin relaxation is dominated by the minority carrier relaxation and the behavior of the electrons (holes) optically created was not accessible. Here we focus our attention on the latter.

We studied the CW luminescence polarization close to the Fermi level in an *n*-type-doped QW for which the second confined electron subband is marginally occupied. Contrary to the expectation, the data revealed that the presence of the electron gas in the first confined electron subband does not completely cancel the spin polarization of the electrons optically created close to the Fermi level in the second subband. On the other hand, we observe that the polarization of these electrons is affected by the electron-hole exchange interaction when the photocarrier concentration is increased.

Our sample is a strained 130 Å -wide *n*-type modulation-doped $Al_{0.25}Ga_{0.75}As/In_{0.2}Ga_{0.8}As/GaAs$ QW. In this system, electron transfer from a Si δ-doping layer placed at 50 Å from the well interface gives rise to a high-density 2D electron gas in the QW region ($N_{2D}=2\times10^{12}$ cm^{-2}). Four conduction subbands are occupied. The second and third subband states, however, are localized in the δ-doping layer. Consequently, their overlap with the first heavy-hole subband (denominated H_1), which is confined in the well region, is weak.[13] Therefore, these subbands do not give significant contributions to optical transitions. Here, we focus our attention on the first and fourth conduction subbands, which are denominated E_1 and E_2 (where the index labels only the conduction states mainly confined in the well region). The Fermi level is almost degenerate with E_2, which is marginally occupied. This allowed us to study the relaxation of electrons under two different situations in the same sample: a highly occupied first conduction subband and a marginally occupied second conduction subband, which correspond to the cases $k_F>0$ and $k_F\approx0$, respectively (where k_F is the electron wave vector at the Fermi energy). In order to compare with more standard situations, we also studied the same sample after a hydrogen (H)-passivation processing[15] when the electron gas density was reduced to

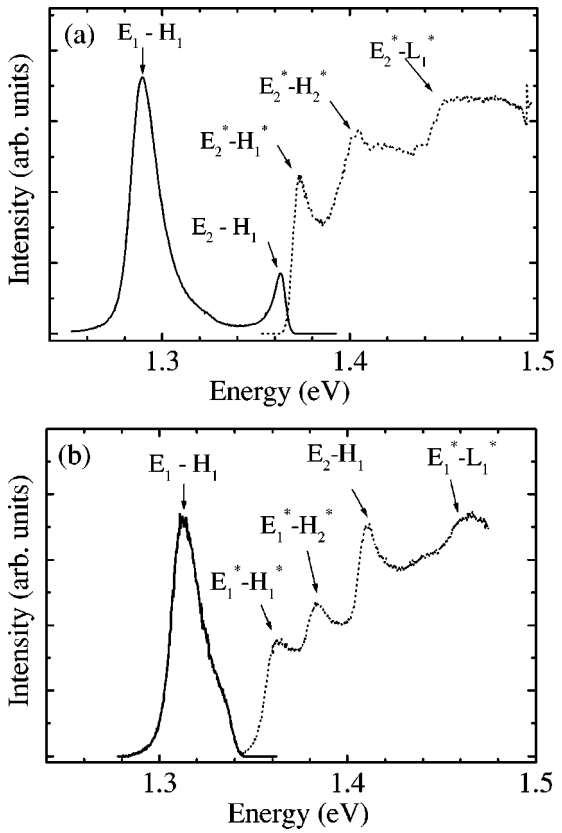

FIG. 1. I_+ PL (solid lines) and PLE (dotted lines) spectra for (a) as-grown sample; (b) H-passivated sample.

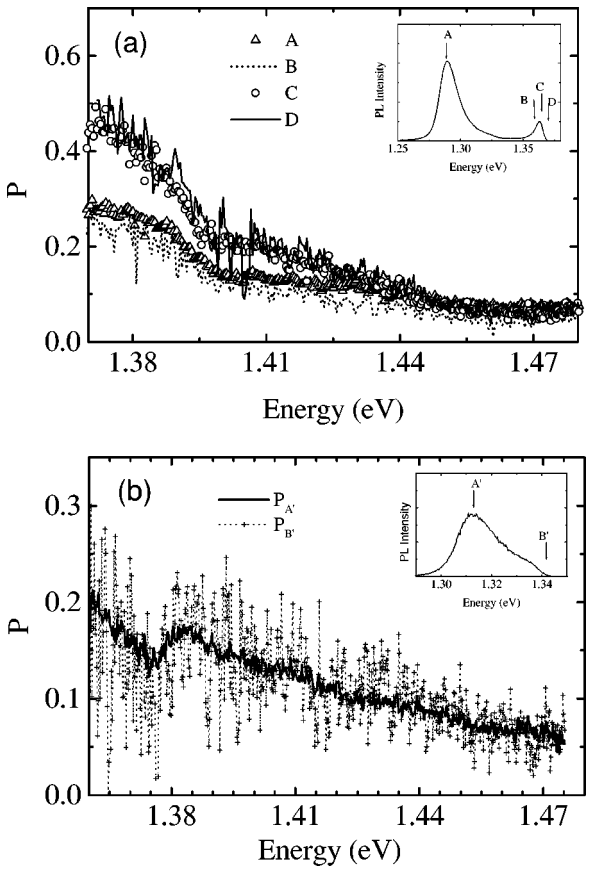

FIG. 2. (a) Polarization profiles for the as-grown sample at the detection energies A, B, C, and D; (b) Polarization profiles for the H-passivated sample at the detection energies A' and B'. The inset shows the respective energy positions.

$N_{2D}=1\times10^{12}$ cm^{-2} lowering the Fermi level well below the second conduction subband.

We performed CW photoluminescence (PL) and photoluminescence excitation (PLE) experiments with circularly polarized light (σ_+ and σ_-) at excitation and detection. The measurements were carried out at $T=14$ K using a cold-finger cryostat. The excitation polarization is kept fixed and I_- and I_+ are, respectively, the PL intensities upon detection at the opposite and at the same polarization as the excitation. The luminescence polarization degree is defined as $P=(I_+ - I_-)/I_+ + I_-$. We investigated P as a function of the excitation and detection energies as well as the excitation intensity.

Figure 1 shows the PL (solid lines) and PLE (dashed lines) spectra for (a) the as-grown sample and (b) the H-passivated sample. In these figures only I_+ is shown. For the as-grown sample the PL spectrum presents two peaks, corresponding to the E_1-H_1 and E_2-H_1 transitions. The PLE peaks are attributed to the $E_2^*-H_1^*$, $E_2^*-H_2^*$ and $E_2^*-L_1^*$ transitions, where H_2 and L_1 are the second heavy-hole and the first light-hole subbands, respectively. These transitions have been identified by comparison with self-consistent calculations.[13] The symbol * indicates that the transition occurs at $k_\parallel=k_F^{(i)}$ while the others occur at $k_\parallel=0$ (where $k_\parallel$ is the in-plane wave vector and $k_F^{(i)}$ is the in-plane wave vector of the ith conduction subband).

The transition $E_1^*-H_1^*$ in the as-grown sample [Fig. 1(a)] is not resolved in the PLE spectrum since it is very close in energy to the $E_2^*-H_1^*$ transition. The E_2-H_1 transition is allowed due to the high built-in electric field created by the asymmetric doping. The 2D electron gas densities were estimated from the Stokes shifts between E_1-H_1 and $E_2^*-H_1^*$ [Fig. 1(a)] or $E_1^*-H_1^*$ [Fig. 1(b)], and they are consistent with the values used in the calculations to give the correct PLE energy transitions. The observed small Stokes shift between $E_2^*-H_1^*$ and E_2-H_1 in Fig. 1(a) indicates that the second subband is slightly occupied. After the passivation processing the Fermi level was shifted below the second confined-electron subband. The PL spectrum exhibits only one peak, corresponding to the E_1-H_1 transition. An abrupt cut in the high-energy luminescence tail in Fig. 1(b) indicates the Fermi energy ($E_1^*-H_1$ transition).

In Fig. 2(a) we show the polarization profiles P_A, P_B, P_C, and P_D for the as-grown sample at the detection energies A, B, C, and D, respectively, as indicated in the inset. These energies correspond to luminescence at the transitions: E_1-H_1 for position A, $E_1^*-H_1$ for position B, E_2-H_1 for position C, and $E_2^*-H_1$ for position D. Figure 2(b) shows the polarization profiles $P_{A'}$ and $P_{B'}$ for the H-passivated sample at the detection energies A' and B' indicated in the inset, corresponding to the transitions at the PL peak E_1-H_1 (position A') and at the Fermi edge $E_1^*-H_1$ (position B'). Note that the luminescence involves the same hole state, H_1. The holes quickly relax to their low-energy states. The alloy scattering breaks the in-plane momentum conservation allowing transitions between electron states with $k_e=k_F$ and hole states at $k_h=0$.

Let us first discuss the results for the as-grown sample [Fig. 2(a)]. All the profiles present the same features: the polarization degree is high for excitation energies slightly above the $E_2^*-H_1^*$ transition and decreases as the excitation energy increases. Pronounced relative loss of polarization is observed at excitation energies around the $E_2^*-H_2^*$ and $E_2^*-L_1^*$ excitations. These results indicate that the polarization *profile* is basically determined by the momentum-dependent hole-spin mixing, since the pronounced losses occur upon excitation of transitions that involve different hole states and the same conduction subband. The biaxial strain induced by the lattice mismatch in this system separates the light-hole subband L_1 from the heavy-hole subbands H_1 and H_2. Consequently, the valence-band mixing is weak at the band edge and the hole spin flip is slowed down. The asymmetric QW structure complicates considerably the calculations of the hole-spin relaxation. The existing theoretical model that takes account of this kind of situation[14] invokes a motional narrowing mechanism involving hole wave-vector scattering. The characteristics of the sample that affects this scattering will determine the polarization profile. A more detailed discussion of the polarization profile is out of the scope of this paper.

The remarkable result of Fig. 2(a) is the difference in the polarization *degree* observed for different detection energies. When the luminescent states involve the first conduction subband (positions A and B) the polarization degree is $P_{A,B}\approx 25\%$ for excitation just above the $E_2^*-H_1^*$ transition. For detection at the second PL peak C and at higher energy D, the polarization degree increases to $P_{C,D}\approx 45\%$ at the same excitation energy. In all cases the polarization degree decays to 5% when the excitation is above the $E_2^*-L_1^*$ transition.

The high-density electron gas in the first conduction subband does not exhibit spin polarization. Therefore, since the luminescence at position A only involves the band-edge states of E_1 and H_1, no spin polarization from the optically created electrons is expected to be observed. All the detected polarization in this case results from the holes that relaxed to the top of the H_1 subband. On the other hand, luminescence at position C involves the second confined subband. The observed enhancement of the polarization degree at position C, with respect to that at position A, results from the presence of spin-polarized electrons in E_2. Despite the presence of the electron gas in E_2, the luminescence from the vicinity of the Fermi level retains, at least partially, the spin polarization of the optically excited electrons in this subband. The degree of spin polarization of the electrons that are recombining at position C, P_C^e, can be obtained approximately from $P_C^e\simeq P_C-P_A$, since the polarization of the participating holes is expected to be the same in the transitions A and C, and in A the electrons are unpolarized. The same result is obtained for the transitions D and B when the electrons involved are those at the Fermi level. Since the carrier concentration in the subband E_2 is very low, the transitions in positions C and D basically involve a mixing of photocreated electrons and electrons from the electron gas.

For the H-passivated sample [Fig. 2(b)] the results do not show any difference either in the polarization profile or in the degree of polarization along the PL spectrum. For this sample, the Fermi energy is well below the E_2 subband. The electrons are optically created just above the E_1^* energy and $P_{B'}^e\simeq P_{B'}-P_{A'}=0$.

Recent calculations in *p-doped* symmetric QW's (Ref. 7) show that the electron spin relaxation in 2D systems is dominated by two mechanisms: the D'Yakonov-Perel' (DP) (Ref. 16) and the Bir-Aronov-Pikus (BAP) (Ref. 17) mechanisms. The DP mechanism arises from the lack of inversion symmetry and from the spin-orbit interaction in the III-V structures, which split the conduction band and mix the electron spin states. The resulting spin splitting has a linear dependence with the electron wave vector $k_\parallel^e$. The relaxation process is a motional-narrowing-type mechanism in which the spin relaxation is slower when the electron momentum relaxation is faster. In the BAP mechanism the spin relaxation process comes from the exchange interaction between conduction electrons and valence holes during the momentum relaxation. Its efficiency is mainly determined by the carrier concentration and the phase space available for the electron-hole scattering. The dependence of electron spin relaxation time with the electron kinetic energy shows a competition between the DP and BAP mechanisms. The DP mechanism, however, dominates the spin relaxation for electrons with small wave vectors, when the phase-space filling of the *p*-type-doped system blocks the BAP process.

In our case, the system is a *n-type-doped* asymmetric QW. For the as-grown sample $k_F^{(1)}\gg 0$ and $k_F^{(2)}\approx 0$. The difference on the polarization degree at the Fermi edge of the two different conduction subbands, P_B and P_D, comes from the fact that positions B and D involve luminescence of states with very different values of in-plane wave vectors. This gives rise to different spin mixing and scattering efficiency. The electrons photocreated with $k_e^{(1)}\gtrsim k_F^{(1)}$ in the first subband relax their polarization more rapidly than those at the second subband with $k_e^{(2)}\gtrsim k_F^{(2)}$. For this sample, this effect implies in $P_D>P_B$ and $P_A=P_B$. For the same reason, we obtain $P_{A'}=P_{B'}$ in the H-passivated sample. More surprising is the fact that $P_C\sim P_D$. The luminescences from these positions involve a mixing of electrons from the gas and those optically excited. The strong polarization in these positions shows the low efficiency for the spin relaxation mechanisms at small in-plane wave vectors and that the electron gas in the first subband has little effect on the photocreated electrons.

Figure 3 shows P_C^e, P_A, and P_C (inset) for two excitation intensities $I=3$ W/cm^2 and 90 W/cm^2. For the low intensity excitation, P_C^e is around 20% at an excitation energy just above the $E_2^*-H_1^*$ transition, decreasing as the excitation energy increases. For sufficiently high excitation energy, P_C^e goes to zero. This behavior can be understood within the framework of the mechanisms described above. Optical excitation close to the Fermi level creates electrons with small $k_\parallel^e$, for which spin mixing is weak. As the excitation energy is increased, states with larger $k_\parallel^e$ are excited, increasing scattering events that enhance the spin relaxation rate.

The degree of polarization P is very sensitive to the excitation intensity. P decreases as the laser intensity increases for all detection energies. For an excitation energy just above the $E_2^*-H_1^*$ transition, P_A decreases from 25% to 10% and P_C decreases from 45% to 15% as the intensity increases

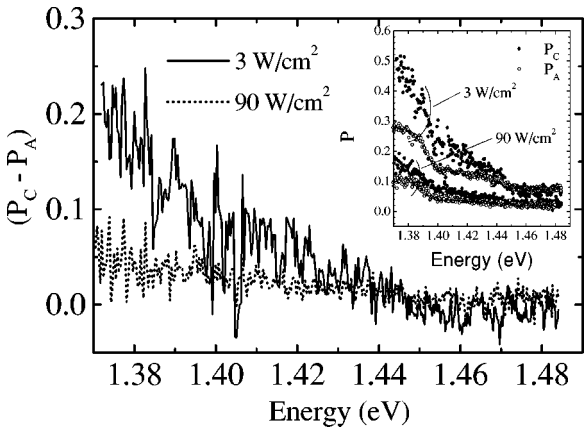

FIG. 3. Electron polarization $P_C^e = P_A - P_C$ of as-grown samples for two excitation intensities: $I = 3$ W/cm^2 and $I = 90$ W/cm^2. Inset: polarization spectra at positions A and C.

from 3 to 90 W/cm^2 (see inset in Fig. 3). This corresponds to relative losses of polarization of $\Delta P_A \approx 60\%$, $\Delta P_C \approx 45\%$, and $\Delta P_C^e \approx 25\%$.[18] The loss of polarization in the vicinity of the Fermi energy occurs, therefore, for holes as well as for electrons. By increasing the excitation intensity one increases the density of photoexcited carriers in the QW. Spin relaxation by motional-narrowing type of mechanisms,[14,16] being enhanced by longer momentum scattering times, are not favored by the more frequent carrier-carrier scattering at high excitation intensity. Consequently the faster hole-spin relaxation observed for high laser power must be related to other spin-flip mechanisms. The best candidate is the hole-hole exchange interaction. This would account for the loss of polarization at the position A and part of that at the position C. Electrons also have a faster spin relaxation at the position C. The electron-electron interaction, however, already occurs at weak laser power due to the presence of the electron gas and shall not change significantly as the excitation intensity increases. On the other hand, electron-hole exchange interaction is now important. The phase-space filling does not play an important role for the electrons in the second subband because it is marginally occupied.

From the above discussion about the hole-spin relaxation mechanisms, only the BAP seems not to have serious restrictions on its efficiency in the investigated system. We believe then that the BAP may be responsible for the observed relative loss of polarization at position C when the laser intensity increases.[19] This conclusion, however, is qualitative and more experimental and theoretical work are necessary for a definitive answer of this problem.

We acknowledge R. G. Pereira and A. L. Gobbi for the H passivation. We are grateful to F. Cerdeira for a critical reading of the manuscript. This work was supported by CNPq, FINEP, CAPES, and FAPESP.

[1] R. C. Miller, D. A. Kleinman, W. A. Nordland, Jr., and A. C. Gossard, Phys. Rev. B **22**, 863 (1980).

[2] T. C. Damen, L. Viña, J. E. Cunningham, J. Shah, and L. J. Sham, Phys. Rev. Lett. **67**, 3432 (1991).

[3] Ph. Roussignol, P. Rolland, R. Ferreira, C. Delalande, G. Bastard, A. Vinattieri, J. Martinez-Pastor, L. Carraresi, M. Colocci, J. F. Palmier, and B. Etienne, Phys. Rev. B **46**, 7292 (1992).

[4] R. Ferreira, Ph. Roussignol, P. Rolland, C. Delalande, A. Vinattieri, and G. Weimann, J. Phys. IV **3**, 175 (1993).

[5] B. Baylac, T. Amand, X. Marie, B. Dareys, M. Brousseau, G. Bacquet, and V. Thierry-Mieg, Solid State Commun. **93**, 57 (1995).

[6] A. L. C. Triques, F. Iikawa, M. Z. Maialle, J. A. Brum, and R. G. Pereira, Superlatt. Microstruct. (to be published).

[7] M. Z. Maialle, Phys. Rev. B **54**, 1967 (1996).

[8] A. E. Ruckenstein, S. Schmitt-Rink, and R. C. Miller, Phys. Rev. Lett. **56**, 504 (1986).

[9] T. Uenoyama and L. J. Sham, Phys. Rev. Lett. **64**, 3070 (1990); Phys. Rev. B **42**, 7114 (1990).

[10] R. Ferreira and G. Bastard, Phys. Rev. B **43**, 9687 (1991).

[11] R. Ferreira and G. Bastard, Europhys. Lett. **23**, 439 (1993).

[12] A. Twardowski and C. Hermann, Phys. Rev. B **35**, 8144 (1987).

[13] M. L. F. Abbade, F. Iikawa, J. A. Brum, Th. Tröster, A. A. Bernussi, R. G. Pereira, and G. Borghs, J. Appl. Phys. **80**, 1925 (1996).

[14] R. Ferreira and G. Bastard, Solid-State Electron. **37**, 851 (1994); Ph. Roussignol, R. Ferreira, C. Delalande, G. Bastard, A. Vinattieri, J. Martinez-Pastor, L. Carraresi, M. Colocci, J. F. Palmier, and B. Etienne, Surf. Sci. **305**, 263 (1995).

[15] S. J. Pearton, Int. J. Mod. Phys. B **8**, 1247 (1994).

[16] M. I. D'yakonov and V. I. Perel', Zh. Eksp. Teor. Fiz. **60**, 1954 (1971) [Sov. Phys. JETP **33**, 1053 (1971)]; M. I. D'yakonov and V. Yu. Kachorowskii, Fiz. Tekh. Poluprovodn. **20**, 178 (1986) [Sov. Phys. Semicond. **20**, 110 (1986)].

[17] G. L. Bir, A. G. Aronov, and G. E. Pikus, Zh. Éksp. Teor. Fiz. **42**, 1382 (1975) [Sov. Phys. JETP **42**, 705 (1975)].

[18] We define relative loss of polarization for the transitions $E_2^* - H_2^*$ and $E_2^* - L_1^*$ as, respectively,

$$\Delta P = \frac{P_{E_2^*-H_1^*} - P_{E_2^*-H_2^*}}{P_{E_2^*-H_1^*}} \quad \text{and} \quad \Delta P = \frac{P_{E_2^*-H_2^*} - P_{E_2^*-L_1^*}}{P_{E_2^*-H_2^*}}.$$

[19] B. Baylac, T. Amand, M. Broussearu, X. Marie, B. Dareys, G. Bacquet, J. Barrau, and R. Planel, Semicond. Sci. Technol. **10**, 295 (1995).